Cerebral Cortex December 2013;23:2840–2854
doi:10.1093/cercor/bhs263
Advance Access publication August 31, 2012

Spatial Stimulus Configuration and Attentional Selection: Extrastriate and Superior Parietal Interactions

Céline R. Gillebert[1], Natalie Caspari[1], Johan Wagemans[2], Ronald Peeters[3], Patrick Dupont[1] and Rik Vandenberghe[1,4]

[1]Laboratory for Cognitive Neurology, [2]Laboratory of Experimental Psychology, University of Leuven, Leuven, Belgium
[3]Department of Radiology, and [4]Department of Neurology, University Hospitals Leuven, Leuven, Belgium

Address correspondence to Rik Vandenberghe, Department of Neurology, University Hospitals Leuven, Herestraat 49 Box 7003, 3000 Leuven, Belgium. Email: rik.vandenberghe@uz.kuleuven.ac.be

The intraparietal sulcus (IPS) is critical for resolving stimulus competition. Its activity is modulated depending on how competing stimuli are spatially configured. Lesions extending into IPS lead to selection deficits when stimuli are configured along a horizontal relative to a vertical or diagonal axis. Using functional magnetic resonance imaging, we examined whether the effect of configuration axis originates at the level of the sensory map in early visual cortex or at the level of the attentional priority map in IPS. In each trial, we presented 1 or 2 peripheral gratings in the upper right visual field and a central letter stream. Subjects performed either a peripheral orientation discrimination task or a central letter detection task. Left IPS activity was higher when peripheral stimuli were configured along the horizontal relative to the vertical axis, but only in peripheral attention conditions. The portions of extrastriate cortex that responded to the peripheral stimuli showed a similar interaction. Connectivity from superior parietal to extrastriate cortex was enhanced by adding a competing distracter during the peripheral attention task. The effect of the spatial configuration between competing stimuli originates at the level of the attentional priority map in IPS rather than the visual sensory map.

Keywords: attention, dynamic causal modeling, extinction, intraparietal sulcus, top-down

Introduction

One of the most striking characteristics of spatial–attentional disorders after right-hemispheric stroke is the strong left-to-right gradient of the deficit (Mesulam 1981). When 2 competing stimuli are presented, patients with right inferior parietal lesions are impaired when the 2 stimuli are configured along a horizontal axis compared with a vertical or a diagonal axis and fail to detect or discriminate the leftmost stimulus (Di Pellegrino and De Renzi 1995; Molenberghs et al. 2008). This effect is present regardless of whether the 2 stimuli are presented symmetrically or asymmetrically. It even occurs for stimuli presented within a same hemifield (Di Pellegrino and De Renzi 1995; Molenberghs et al. 2008).

The configuration axis also modulates brain activity levels in healthy subjects: In the intact brain, the activity levels in the middle segment of the intraparietal sulcus (IPS) are higher when competing stimuli are on a same horizontal axis than when they are configured along the vertical or along the diagonal axis (Molenberghs et al. 2008). This effect occurs for stimulus pairs positioned bilaterally on the horizontal axis versus unilaterally on the vertical axis, for stimulus pairs positioned bilaterally along the horizontal versus the diagonal configuration axis, and for unilateral stimulus pairs presented along the horizontal versus the vertical configuration axis within the same hemifield (Molenberghs et al. 2008). Previous studies of divided attention have described behavioral differences due to the position of 2 stimuli in a single versus both hemifields (Hung et al. 2005, 2011; Kraft et al. 2011). By placing the stimuli within a same hemifield for both the horizontal and the vertical configurations, the effect of configuration axis can be de-confounded from the effect of bilaterality (Molenberghs et al. 2008). The origin of the effect of configuration axis on IPS activity levels is still unclear. Here, we contrasted 2 possibilities. Using functional magnetic resonance imaging (fMRI), we investigated whether the effect of configuration axis arises at the level of the sensory map or at the level of the attentional priority map.

The effect of configuration axis could originate at the level of the sensory map in early visual cortex: According to lateral masking studies (Polat and Sagi 1994; Pavlovskaya et al. 1997), long-distance interactions between Gabor patches depend on alignment axis and stimulus orientation. Contextual interactions in perception have their counterpart in the response properties of V1 (e.g. Gilbert and Wiesel 1990; Kastner et al. 1997; Polat et al. 1998). Converging evidence from anatomical, imaging, and electrophysiological studies (Ts'o et al. 1986; Gilbert and Wiesel 1989; Malach et al. 1993) suggests that contextual interactions are mediated by long-range horizontal connections between cells with non-overlapping receptive fields and similar orientation preference. If the effect of configuration axis in humans arises at the level of the sensory map of perceptual inputs, one would expect to find this effect in early visual cortex even when the stimuli are behaviorally irrelevant. In that case, the modulation of IPS activity by configuration axis could reflect an attentional effect to counteract the sensory effect of configuration axis arising in upstream visual areas. In a previous study (Molenberghs et al. 2008), we did not observe a sensory effect of configuration axis on activity levels in IPS or in early visual cortex when subjects were engaged in a central attention task, and the peripheral stimuli in the configuration were irrelevant. In the present study, we aimed to increase the sensitivity for detecting a sensory effect of configuration axis in retinotopically organized visual areas: We presented stimuli at fixed locations within one quadrant of the visual field and assessed the effect of configuration axis in the portions of early visual cortex that responded to the stimuli, as determined by independent localizer scans. By restricting the possible stimulus locations to 4 fixed eccentric locations within a same quadrant, we maximized sensitivity for detecting early visual effects of sensory stimulation and configuration axis. Restricting the spatial–attentional set to 4 peripheral locations and 1 central location

also kept the working memory demands within a feasible range (Woldorff et al. 2004). To ensure that attentional resources were fully taken up during the sensory control conditions, subjects performed a demanding letter detection task on a foveal letter stream.

Alternatively, the effect of configuration axis may originate at the level of the "attentional priority map", a topographical representation of the environment in which each perceptual input is weighted by its current behavioral relevance (Bundesen 1990; Itti and Koch 2000; Vandenberghe and Gillebert 2009; Bisley and Goldberg 2010). In that case, the effect of configuration axis may originate from areas known to play a role in compiling attentional priorities, such as IPS (Molenberghs et al. 2008; Gillebert et al. 2011) or the frontal eye fields (FEF; Thompson et al. 2005; Wardak et al. 2006; Buschman and Miller 2007; Monosov and Thompson 2009). For instance, the spatial resolution of the attentional priority map and the subjective distance between 2 stimuli may differ between the horizontal and vertical dimension. In particular, it may be more difficult to resolve stimulus competition if the stimuli are configured along the horizontal than vertical axis, even if the physical distance is matched. In the current study, we manipulated the configuration axis and the behavioral relevance of the stimuli within the same experiment: We assessed whether horizontally or vertically configured stimuli yielded differential effects on IPS activity levels when attention was directed toward the stimuli or away from the stimuli. To further test our hypothesis regarding the origin of the effect of configuration axis, we also examined whether the presence of competing stimuli and the configuration axis between competing stimuli modulated the feedforward or the feedback connectivity between early visual cortex and middle IPS using dynamic causal modeling (DCM; Friston et al. 2003).

As a last step, we determined the generalizability of the effect of configuration axis. In previous experiments, subjects performed an orientation discrimination task with a peripheral grating, which was presented simultaneously with an irrelevant grating (Geeraerts et al. 2005; Vandenberghe et al. 2005; Molenberghs et al. 2008; Gillebert et al. 2011). To exclude that the effect of stimulus configuration is specific for oriented gratings as stimuli (Polat and Sagi 1994; Pavlovskaya et al. 1997), we examined the effect of configuration axis on IPS activity levels when subject performed a discrimination task on colored patches instead of oriented gratings.

Materials and Methods

Subjects

We conducted 2 behavioral and 4 fMRI experiments in a total of 53 healthy subjects. Subjects were strictly right-handed, reported normal or corrected-to-normal vision, were free of psychotropic and vasoactive medication, and had no neurological or psychiatric history. Ten subjects (6 women/4 men, aged 20–24) participated in the first behavioral experiment, and 10 subjects (7 women/3 men, aged 20–27) in the second behavioral experiment. Twenty-two other subjects (14 women/8 men, aged 19–32) participated in the first fMRI experiment ("main fMRI experiment") and 6 of them (5 women/1 man, aged 21–24) also in a second fMRI experiment ("sensory fMRI experiment"). Five additional subjects (3 women/2 man, aged 20–38) participated in a third fMRI experiment ("hemifield fMRI experiment"), and 6 additional subjects (3 women/3 men, aged 22–32) in a fourth fMRI experiment ("color fMRI experiment"). All subjects gave written informed consent in accordance with the Declaration of Helsinki. The study was approved by the Ethics Committee, University Hospitals Leuven.

Behavioral Experiments

Stimuli and Experimental Paradigm

Stimulus presentation and response registration were controlled by a personal computer (PC) running Presentation 11.3 (Neurobehavioral systems, Albany, CA, United States of America). All experiments were performed under covert attention conditions. Participants were seated at 50 cm from a 19-inch cathode ray tube monitor (resolution 1024 × 768 pixels, refresh rate 75 Hz) in a dimly lit room. Gaze fixation was monitored on-line by means of infrared eye monitoring (View-Point Eye Tracker; Arrington Research; Scottsdale, AZ, United States of America).

In the first behavioral experiment, subjects performed an orientation discrimination task on a circular grating presented in the peripheral visual field (Fig. 1*A*). Each trial started with a temporal warning cue (diameter 1°; 350 ms), followed by a central white digit cue (size 1.3°; 200 ms). The digit (1, 2, 3, or 4) referred to 1 of the 4 pre-coded target locations, corresponding to the corners of an imaginary square in the upper right visual field (1: Upper left corner; 2: Upper right corner; 3: Lower right corner; 4: Lower left corner). The imaginary square was located on the diagonal, with the upper left and lower right corner at 7.3° eccentricity, the upper right corner at 9.7°, and the lower left corner at 4.1° eccentricity. After a brief delay (diameter fixation point 0.4°; 200 ms), a target grating (200 ms, 2.5° diameter, 0.5 cycles/degree; mean luminance, 19.2 cd/m2) was presented at the cued location. In 66% of the trials, the target was accompanied by a distracter. Target and distracter were configured along the horizontal axis or along the vertical axis, each in 33% of the trials. Each possible location was occupied equally frequently during each event type. The intertrial interval was fixed to 2250 ms. Subjects received 144 training trials prior to the experiment, followed by 5 runs of the 144 trials separated by a brief pause. Each of the conditions (single grating, horizontal configuration, vertical configuration) was repeated 48 times in each run. Subjects held 2 response buttons in their right hand and had to decide whether the target orientation was rotated clockwise or counter-clockwise with respect to a 45° reference orientation. Per run and per condition, these 2 alternatives occurred with equal frequency. The orientation difference (relative to 45°) was adapted on-line from run to run to obtain an average performance level between 70% and 80% correct. The distracter orientation was either congruent or incongruent with the target orientation (in 33% and 66% of the double-stimulation trials, respectively). When incongruent, the distracter orientation was equally often rotated clockwise or counter-clockwise compared with the target orientation.

In the second behavioral experiment (Fig. 1*A*), we investigated whether the behavioral effect of configuration axis was dependent upon the use of gratings in an orientation discrimination task. The experimental design was identical to the first behavioral experiment, but the gratings were replaced by color patches and subjects performed a color discrimination task: They were instructed to press 1 of the 2 buttons depending on the color of the circle at the attended location (ranging from red to yellow, not matched for luminance). In case of 2 colored patches, we manipulated the axis of configuration between target and distracter. The color difference (relative to orange: red, green, blue = 255,128,0) was adapted on-line to reach an average performance between 70% and 80% correct. Each of the 3 conditions (single color path, horizontal configuration, vertical configuration) was shown 48 times in each run, and 288 times in the whole experiment (6 runs).

Analysis of Performance

For each subject and each condition in the experimental design, we calculated 2 measures of performance: d' (Macmillan and Creelman 1991), the ability to discriminate between 2 grating orientations, and the average reaction time (RT) on correct trials. Data were analyzed

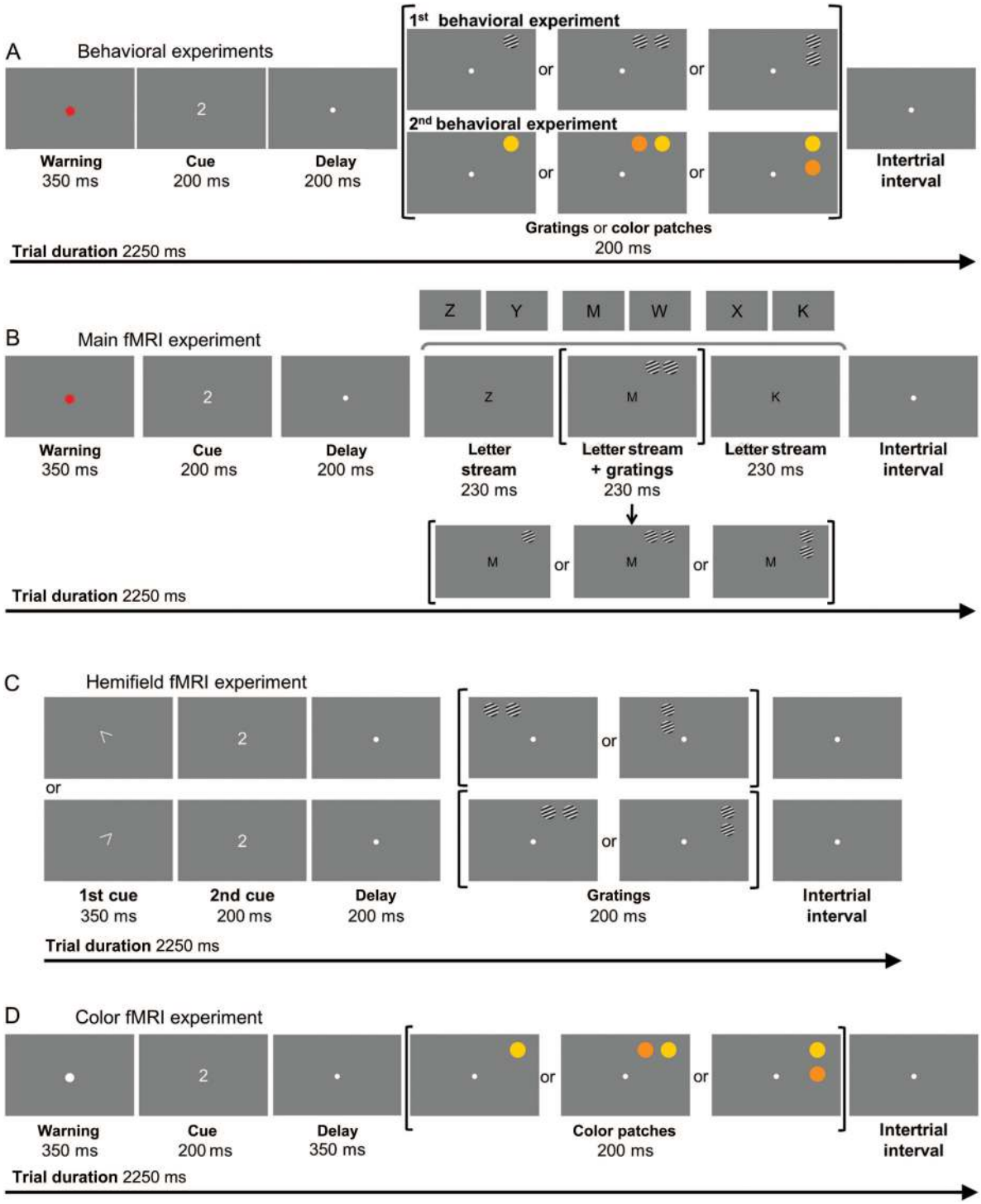

Figure 1. Experimental paradigm. (*A*) In the behavioral experiments, a digit cued attention to a location in the upper right visual field. The target at the cued location was presented either on its own or simultaneously with a competing distracter. In that case, target and distracter were configured along the horizontal or the vertical axis. (*B*) In the main fMRI experiment, we simultaneously presented a central letter stream and peripheral gratings. Subjects were instructed to determine whether or not the letter stream contained the letter X, or to discriminate the orientation of the grating presented at the target location. In each trial, 1 or 2 gratings were presented in the upper right visual field. In case of 2 gratings, they were configured along the horizontal or the vertical axis. (*C*) In the hemifield fMRI experiment, oriented gratings appeared in the right upper visual field or in the left upper visual field. The target at the cued location was always presented simultaneously with a competing distracter. Target and distracter were configured along the horizontal or the vertical axis. (*D*) In the color fMRI experiment, the target at the cued location was presented either on its own or simultaneously with a competing distracter. In that case, target and distracter were configured along the horizontal or the vertical axis.

using a repeated-measures analysis of variance (ANOVA) with stimulus display (single target, double horizontal, double vertical) as factor. When sphericity could not be assumed (Mauchly's sphericity test: $P < .05$), *P*-values were adjusted using the Greenhouse–Geisser correction (G–G adj.). A priori comparisons included the contrast between double stimulation and single stimulation, and between

horizontal and vertical configuration axis in the case of double stimulation. In the behavioral experiments, the eye movement recordings were not formally analyzed for technical reasons.

fMRI Experiments

Stimuli and Experimental Paradigms

Stimulus presentation and response registration were controlled by a PC running Presentation 11.3 (Neurobehavioral systems). All experiments were performed under covert attention conditions. Stimuli were projected onto a translucent screen in front of the subject by means of a liquid crystal display projector (1024 × 768 pixels, 75 Hz; Barco 6400i; Barco, Kortrijk, Belgium). The eccentricity of the peripheral stimuli was identical to that in the behavioral experiments. Eye movements were registered using an Applied Science Laboratory infrared system (ASL 5000/LRO system; Waltham, MA, United States of America) and stored for subsequent quantitative analysis.

In the first fMRI experiment ("main fMRI experiment"), we determined the effect of task relevance (central letter detection vs. peripheral orientation discrimination) on the effect of configuration axis (horizontal vs. vertical). Each trial (duration 2250 ms) started with an instructive color cue (350 ms), red or green. The color indicated whether subjects had to discriminate the orientation of the spatially cued peripheral grating or, alternatively, conduct a central letter detection task (Fig. 1*B*). This was followed by a central spatial cue (size 1.3°; 200 ms), consisting of a digit ranging from 1 to 4 referring to 1 of the 4 pre-coded possible grating locations. After a 200-ms delay, a foveal 6-letter stream was initiated (size 1.3°; letter-to-letter onset asynchrony 115 ms, letter duration 65 ms). The letters were pseudorandomly chosen from a limited set (KMNVWXYZ), with the constraint that 2 subsequent letters were never identical and that a target letter "X" was present in half of the trials. Simultaneously with the onset of the third letter, 1 or 2 peripheral gratings (in either a horizontal or a vertical configuration) were presented for 230 ms at the corners of an imaginary square on the diagonal in the right upper quadrant (Fig. 1*B*). As in the behavioral experiment, the distracter orientation was either congruent or incongruent with the target orientation (in 33% and 66% of the double-stimulation trials, respectively). When incongruent, the distracter orientation was equally often rotated clockwise or counter-clockwise compared with the target orientation. Subject held 2 response buttons in their right hand. During the peripheral attention conditions, they had to direct their attention to the cued grating and select a key press response depending on the cued grating's orientation. During the central attention conditions, they were instructed to select a key press response depending on whether or not the letter stream contained an X (Fig. 1*B*). In each run, the 6 event types in the 2 × 3 experimental design (task × stimulus configuration) were each shown 24 times and randomly intermixed with 24 null events (Wager and Nichols 2003). All subjects performed 6 runs in total.

We conducted a second fMRI experiment ("sensory fMRI experiment") to delineate the sensory response to the peripheral stimuli in early visual cortex. We presented 0, 1, or 2 (in either a horizontal or a vertical configuration) gratings in the upper right quadrant of the visual field. Each corner of the imaginary square in the upper right visual field was occupied equally often in each condition. Subjects performed the central letter detection task throughout the experiment. The initial cue always had a fixed color (green), and the spatial cue was omitted. Each of the 4 event types (no gratings, single grating, horizontal configuration, and vertical configuration) was presented 36 times in each run. Two subjects performed 5 runs, 4 subjects 6 runs. In each run, the order of the 4 conditions was pseudorandomized (Wager and Nichols 2003), and task trials were intermixed with 24 null events.

In a third fMRI experiment ("hemifield fMRI experiment"), we determined to which degree results obtained in the main experiment were dependent on the location of the gratings in the right upper quadrant. The experimental design was factorial with 2 factors: Stimulus configuration (horizontal vs. vertical) and stimulus position (left vs. right upper quadrant). This experiment only contained peripheral attention trials in which a target and a distracter grating were presented. The central spatial cue consisted of an arrow indicating whether the stimuli would appear in the left or the right upper quadrant (duration 300 ms), followed by a digit, indicating in which of the 4 possible positions the target would appear (duration 200 ms). The central spatial cue was followed by a delay interval (duration 200 ms) and presentation of the 2 gratings (duration 200 ms; Fig. 1*C*). Subjects had to discriminate the orientation of the cued grating. In half of the trials, this pair of gratings appeared in the right upper quadrant, identically to the main experiment, and in the other half in the left upper quadrant, at positions symmetrical to those used in the right upper quadrant (Fig. 1*C*). In each run, the 4 event types (horizontal configuration/upper left visual field, vertical configuration/upper left visual field, horizontal configuration/upper right visual field, vertical configuration/upper right visual field) were each shown 36 times and randomly intermixed with 24 null events. All subjects performed 6 runs.

In a fourth fMRI experiment ("color fMRI experiment"), we replaced the gratings by colored patches (2.5° diameter; Fig. 1*D*). Subjects had to determine the color of the patches. The initial cue always had a fixed color (white). No letters were presented at the fovea. All subjects performed 6 runs. In each run, the 3 event types (single color patch, horizontal configuration, vertical configuration) were each shown 48 times and randomly intermixed with 24 null events.

The term "stimulus display" will be used to refer to all 3 stimulus conditions, that is, single peripheral stimulus, horizontal configuration, and vertical configuration. The term "configuration axis" will be used to refer to 2 of these conditions: Horizontal configuration and vertical configuration.

Image Acquisition

The fMRI experiments were run in a 3T Philips Intera magnet with an 8-channel sensitivity encoding (SENSE) head coil. The whole-brain functional scans consisted of T_2* gradient-echo echoplanar images (EPIs) acquired continuously in an ascending order (6 runs, 189 scans per run, 2000-ms repetition time [TR], 30-ms echo time [TE], 80 × 80 acquisition matrix, 2.75 × 2.75 mm^2 in-plane resolution, 36 3.75-mm thick axial slices without gap). We also acquired a T_1-weighted anatomical image (9.6 ms TR, 4.6 ms TE, 256 × 256 acquisition matrix, 1 × 1 mm^2 in-plane resolution, 182 coronal slices with 1.2 mm thickness).

Analysis of Behavioral Data From the fMRI Experiments

RTs in the different conditions were calculated from grating onset. Behavioral data obtained during the main fMRI experiment were analyzed using a repeated-measures ANOVA with stimulus display (3 levels: Single grating, horizontal configuration, vertical configuration) and task (2 levels: Central letter detection, peripheral orientation discrimination) as factors. A priori contrasts included the interaction between task and double- versus single-stimulation, and between task and configuration axis (horizontal vs. vertical). Behavioral data obtained during the sensory fMRI experiment were analyzed using a 1-way ANOVA with peripheral sensory stimulation as within-subject factor (4 levels: No gratings, single grating, horizontal configuration, vertical configuration). Behavioral data obtained during the hemifield fMRI experiment were analyzed using a repeated-measures ANOVA with hemifield (2 levels: Upper left visual field, upper right visual field) and configuration axis (2 levels: Horizontal configuration, vertical configuration) as within-subject factors. Behavioral data obtained during the color fMRI experiment were analyzed using a repeated-measures ANOVA with stimulus display as factor (3 levels: Single color patch, horizontal configuration, vertical configuration). When sphericity could not be assumed (Mauchly's sphericity test: $P < 0.05$), P-values were adjusted using the Greenhouse–Geisser correction (G–G adj.).

To analyze eye movements, we defined a region of interest that covered a rectangular area in the upper right quadrant of the visual field, with the inner corner at 1° eccentricity and the outer corner at 9° eccentricity. Deviations of eye movements into that region of interest were detected automatically and calculated. For the main fMRI experiment, deviations of eye movements into that region of interest were submitted to a repeated-measures ANOVA with task (2 levels:

Peripheral orientation discrimination task, central letter detection task) and stimulus display (3 levels: Single grating, horizontal configuration, vertical configuration) as factors. A comparable approach was adopted for the analysis of the eye movements in the sensory fMRI experiment, the hemifield fMRI experiment, and the color fMRI experiment.

Analysis of the fMRI Data

Preprocessing and statistical analysis were performed with Statistical Parametric Mapping (SPM) 5 (Wellcome Trust Centre for Neuroimaging, London, United Kingdom, http://www.fil.ion.ucl.ac.uk/spm). The EPIs were corrected for differences in acquisition time, realigned to correct for head movements, and co-registered to the T_1-weighted image. The T_1-weighted image was warped into the Montreal Neurological Institute (MNI) space (via the segmentation option in SPM), and the resulting transformation was used to spatially normalize the functional images. The voxel size of the images in MNI space was $3 \times 3 \times 3$ mm^3. The images were spatially smoothed with a $5 \times 5 \times 7$ mm^3 full-width half-maximum kernel. For each analysis, we included the 6 motion regressors. The hemodynamic response was modeled using the canonical hemodynamical response function in SPM.

Main fMRI Experiment

We modeled the fMRI data using a general linear model (GLM) with 6 main regressors, coding for each combination of task (peripheral task, central task), and stimulus display (single grating, horizontal configuration, vertical configuration). The primary contrasts (contrasts 1–5) were based on comparisons between the double-stimulation conditions:

- Contrast 1: Peripheral task "minus" central task, and the reverse: [(Peripheral task/horizontal configuration + peripheral task/vertical configuration) – (central task/horizontal configuration + central task/vertical configuration)].
- Contrast 2: Horizontal configuration "minus" vertical configuration, and the reverse: [(Peripheral task/horizontal configuration + central task/horizontal configuration) – (peripheral task/vertical configuration + central task/vertical configuration)].
- Contrast 3: Interaction between task and configuration axis, and the reverse: [(Peripheral task/horizontal configuration – peripheral task/vertical configuration) – (central task/horizontal configuration – central task/vertical configuration)].
- Contrast 4: Simple effect of configuration axis in the peripheral task: (Peripheral task/horizontal configuration – peripheral task/vertical configuration).
- Contrast 5: Simple effect of configuration axis in the central task: (Central task/horizontal configuration – central task/vertical configuration).
- Contrast 6: Double stimulation "minus" single stimulation: [(Peripheral task/horizontal configuration + central task/horizontal configuration) + (peripheral task/vertical configuration + central task/vertical configuration) – (peripheral task/single grating + central task/single grating)].
- Contrast 7: All task trials "minus" baseline: [(Central task/single grating + central task/horizontal configuration + central task/vertical configuration) + (peripheral task/single grating + peripheral task/horizontal configuration + peripheral task/vertical configuration) – baseline].

Contrast images were calculated for each subject and evaluated at the second level using 1-sample *t*-tests (voxel-level $P < 0.005$, cluster-level FWE-corrected $P < 0.05$). Significant interactions (contrast 3) were further characterized by means of simple effects (contrasts 4 and 5). Statistical significance for the simple effects was Bonferroni-corrected for multiple comparisons (corrected $P < 0.05$).

Sensory fMRI Experiment

We modeled the fMRI data using a GLM with 4 main regressors (no gratings, single grating, horizontal configuration, vertical configuration). At the single-subject level, we calculated:

- Contrast 8: [(Single grating + horizontal configuration + vertical configuration)/3 – no gratings].

All voxels in occipital cortex that reached whole-brain FWE-corrected $P < 0.05$ in a given subject in this contrast were included in this subject's volume-of-interest (VOI). Within this subject-specific VOI, the time course of the blood oxygen level–dependent (BOLD) response was extracted for each condition, averaged across all runs and all voxels in the VOI. This VOI-based approach allowed us to maximize sensitivity for detecting sensory effects compared with a whole-brain search and to account for between-subject variability. Using a paired *t*-test, we evaluated whether the peak % signal change relative to fixation was different for horizontal configuration versus vertical configuration. Next, we extracted from the main fMRI experiment in the same 6 subjects in the subject-specific VOI the time course under central and peripheral attention conditions. We analyzed the % signal change using a repeated-measures ANOVA with task (central letter detection vs. peripheral orientation discrimination) and configuration axis (horizontal configuration vs. vertical configuration) as within-subject factors.

Hemifield fMRI Experiment

We modeled the fMRI data using a GLM with 4 main regressors (left upper quadrant/horizontal configuration, left upper quadrant/vertical configuration, right upper quadrant/horizontal configuration, right upper quadrant/vertical configuration). Within the regions that showed a significant interaction effect in the main experiment (contrast 3; threshold: Voxel-level $P < 0.005$, cluster-level FWE-corrected $P < 0.05$), we evaluated the interaction between hemifield and configuration axis on activity levels. We analyzed the peak % signal change in these VOIs using a repeated-measures ANOVA with hemifield (left vs. right upper quadrant) and configuration axis (horizontal vs. vertical) as within-subject factors.

Color fMRI Experiment

We modeled the fMRI data using a GLM with 3 main regressors (single color patch, horizontal configuration, vertical configuration). We evaluated the effect of configuration axis on activity levels within the regions that showed a significant interaction effect in the main fMRI experiment (contrast 3; threshold: Voxel-level $P < 0.005$, cluster-level FWE-corrected $P < 0.05$). We analyzed the peak % signal change in these VOIs using a repeated-measures ANOVA with hemisphere (left hemisphere vs. right hemisphere) and configuration axis (horizontal vs. vertical) as within-subject factors. The analysis was limited to double-stimulation trials.

DCM: Main Analysis

Using DCM, we investigated how the addition of a distracter affected connectivity between IPS and up-stream visual areas and how this differed depending on task and configuration axis. The GLM used to extract the relevant time series for DCM (Stephan et al. 2007) consisted of the external input term and 5 regressors: Single grating/peripheral task (Sp), horizontal configuration/peripheral task (Hp), vertical configuration/peripheral task (Vp), horizontal configuration/central task (Hc), and vertical configuration/central task (Vc). The external input term modeled the onset of all trials and this was identical for each DCM model. The 5 regressors were used as modulations on the connections (see later). Note that adding the single grating/central task as a 6th regressor would induce a strict linear dependence between input and regressors and is therefore not permitted.

The node in left middle IPS corresponded to the cluster obtained in the interaction contrast in the fMRI main experiment (contrast 3; random effects analysis, threshold: Voxel-level $P < 0.005$, cluster-level FWE-corrected $P < 0.05$, Table 1D, Fig. 5*F*). The node in extrastriate cortex corresponded to the occipital cluster obtained in the sensory fMRI experiment (contrast 8; random effects analysis, voxel-level $P < 0.001$, cluster-level FWE-corrected $P < 0.05$, Table 2B, Fig. 7*A*). Each node contained the same voxels for all subjects, similarly to the procedure we applied in previous DCM analyses (Van Doren et al. 2010).

Table 1
Main fMRI experiment

Region	*x*	*y*	*z*	*Z* (peak)	Extent (voxels)	*P*-value (FWE-corrected)
(A) Effect of task in double-stimulation trials: Peripheral orientation discrimination versus central letter detection						
Bilateral IPS	15	−63	54	6.28	3525	<0.001
	−30	−81	27	6.36		
Right FEF	27	6	60	5.15	306	<0.001
Left FEF	−27	−6	51	5.68	480	<0.001
Right thalamus	15	−27	15	3.79	79	0.006
Left thalamus	−18	−30	6	4.78	189	<0.001
Left IFG	−48	27	30	4.01	238	<0.001
(B) Effect of task in double-stimulation trials: Central letter detection versus peripheral orientation discrimination						
Left LOC	−36	−87	−6	6.19	238	<0.001
Right LOC	36	−90	0	5.88	333	<0.001
Left STG	−54	−36	24	5.44	326	<0.001
Right STG[a]	63	−21	21	5.08	212	<0.001
Right IFG[a]	54	24	0	4.62	318	<0.001
Right MTG[a]	51	−18	−9	4.50	69	0.013
Right ACC[a]	9	39	15	3.78	69	<0.001
(C) Effect of configuration axis in double-stimulation trials						
Right IPS	30	−63	36	3.89	79	0.005
Right FEF	33	6	60	4.51	145	<0.001
Right MFG	33	36	21	4.40	191	<0.001
Right thalamus	9	−21	6	4.05	71	0.009
Left FEF	−30	0	54	3.84	73	0.008
Left LG[a]	−9	−81	−3	4.08	102	0.001
(D) Interaction between task and configuration axis						
Left IPS	−24	−57	51	3.60	93	0.001
Left FEF	−21	−6	66	4.57	93	0.001
DMPFC	−3	12	51	3.74	84	0.003
Left NC[a]	−9	6	9	4.44	62	0.016
Medial visual[b]	−12	−75	9	4.02	441	<0.001
PCC[a]	12	−42	48	3.77	74	0.006

Note: Stereotactic MNI coordinates of brain areas showing (A and B) a significant main effect of task in the case of double-stimulation trials (contrast 1 and the reverse), (C) a significant main effect of configuration axis (contrast 2), and (D) a significant interaction between task and configuration axis (contrast 3). Threshold: Voxel-level uncorrected $P < 0.005$, cluster-level FWE-corrected $P < 0.05$.
Extent, $3 \times 3 \times 3$ mm^3 voxels; IPS, intraparietal sulcus; LG, lingual gyrus; FEF, frontal eye fields; MFG, middle frontal gyrus; IFG, inferior frontal gyrus; LOC, lateral occipital complex; STG, superior temporal gyrus; ACC, anterior cingulate cortex; DMPFC, dorsomedial prefrontal cortex, NC, nucleus caudatus; PCC, posterior cingulate cortex.
[a]The effect was due to a differential decrease between conditions compared with baseline and will not be further discussed.
[b]The medial visual cluster encompassed left and right lingual gyrus, calcarine gyrus, middle occipital gyrus, and cuneus.

Table 2
Sensory fMRI experiment: Stereotactic MNI coordinates of occipital brain areas showing a significant activity increase when 1 or 2 gratings were presented in the upper right quadrant of the visual field under foveal attention conditions (contrast 8)

Subject	*x*	*y*	*z*	*Z* (peak)	Extent (voxels)
(A) Subject-specific level					
Subject 1	−18	−75	−9	>7.84	84
Subject 2	−6	−81	−6	>7.84	209
Subject 3	−21	−72	−3	>7.84	261
Subject 4	−24	−72	−15	>7.84	93
Subject 5	−21	−75	−9	>7.84	77
Subject 6	−9	−78	−12	>7.84	173
(B) Random effects analysis					
Group	−12	−78	−3	4.07	36

The intrinsic connections (Friston et al. 2003) reflect the influence of one region on another region in the absence of the modulation by experimental effects and consisted of a feedforward and a feedback connection between extrastriate cortex and IPS. The models differed in terms of which of these intrinsic connections were modulated and in terms of the modulating factors (Fig. 2). In model 1, the 3 peripheral task conditions modulated the feedforward connection; in model 2, they modulated the feedback connection; and in model 3, both the feedforward and the feedback connection. Models 4–6 were analogous except for the replacement of the horizontal configuration/peripheral task and the vertical configuration/peripheral task conditions with the horizontal configuration/central task and the vertical configuration/central task conditions, respectively. These models were included to evaluate how specific the effects were for the peripheral attention conditions.

From the data in the main fMRI experiment ($n = 22$), we calculated the principal eigenvariate of the time series in each voxel of each of these VOIs, adjusted for the effect of interest. The average of this eigenvariate over all voxels of each VOI was used for the DCM analysis. The parameters of the hemodynamic response were adjusted for 3T magnetic field strength based upon the values reported by Mildner et al. (2001) and Dupont et al. (2011). We formally compared the models at the subject-specific level by means of the Bayes factor (BF), which is based on the Akaike (AIC) and the Bayesian information criterion (BIC). Following the classification by Raftery (1995; weak evidence: $1 < BF < 3$, positive evidence: $3 < BF < 20$, strong evidence: $20 < BF < 150$, very strong evidence: $BF \geq 150$), a selection between models was made if the BF was at least 3 ("positive evidence"). To compare the models at the group level, we calculated the group Bayes factor (GBF; Penny et al. 2004). To evaluate between-subject consistency, we additionally computed the positive evidence ratio (PER): PER is the number of subjects in whom the evidence is in favor of model A compared with the number of subjects in whom the evidence is in favor of model B (Stephan et al. 2007).

The subject-specific intrinsic couplings and modulatory effects of the best fitting model were entered into separate 1-sample *t*-tests (2-sided, statistical threshold: $P < 0.05$, Bonferroni-corrected for multiple comparisons). To test the hypothesis that the strength of the modulation differed between conditions, the modulatory parameters were entered into paired *t*-tests.

DCM: Confirmatory Analysis
We performed a second DCM analysis to test the robustness of the DCM results with regards to the exact definition of the regressors and of the nodes. External input and intrinsic connections were identical to those of the main DCM. In this confirmatory analysis, the first regressor corresponded to all horizontal configuration trials and the second regressor to all peripheral task trials with horizontal configuration. In model 1, the 2 regressors modulated the feedforward connection between left extrastriate cortex and left IPS; in model 2, the feedback connection; and in model 3, both the feedforward and the feedback connection (Fig. 3). The extrastriate and the IPS node were defined per individual based on the contrast between all trials versus baseline (contrast 7, uncorrected $P < 0.005$). We started from the local maximum in the individual's activation map that was the closest to the group local maximum. All voxels that lay within 6 mm from this individual's local maximum and survived an uncorrected $P < 0.005$ threshold were included in the individual's VOI. The time series were extracted as the first eigenvariate of this VOI.

Results

Behavioral Performance

Behavioral Experiments
In the first behavioral experiment (Fig. 1*A*), the main effect of stimulus display on behavioral performance was significant (d': $F_{2,18} = 16.87$, $P < 0.001$; RTs: $F_{2,18} = 80.96$, $P < 0.001$; Fig. 4*A*,*B*): Subjects responded significantly more slowly ($F_{1,9} = 95.78$, $P < 0.001$) and less accurately ($F_{1,9} = 26.30$, $P < 0.001$) when a distracter was presented together with a target compared with the target-only condition. Furthermore, RTs were longer when target and distracter were configured along the horizontal relative to the vertical axis (RTs: $F_{1,9} = 12.39$, $P = 0.007$; d': $F_{1,9} = 1.34$, $P = 0.28$).

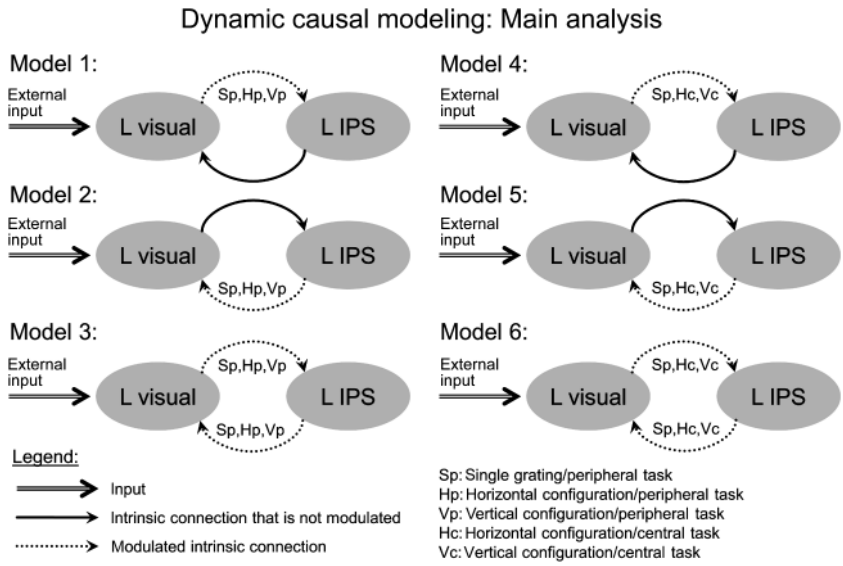

Figure 2. DCM: Main analysis. Six models for the DCM model comparison. Black arrows represent intrinsic connections. Thick and solid black arrows are intrinsic connections for which the model does not contain modulating factors, dotted black arrow connections for which the model contains modulating factors. The GLM used to extract the relevant time series for the 6 DCMs consisted of the external input term and 5 regressors: Single grating/peripheral task (Sp), horizontal configuration/peripheral task (Hp), vertical configuration/peripheral task (Vp), horizontal configuration/central task (Hc), and vertical configuration/central task (Vc). The external input reflect the trial onsets across all trial types and was identical between models.

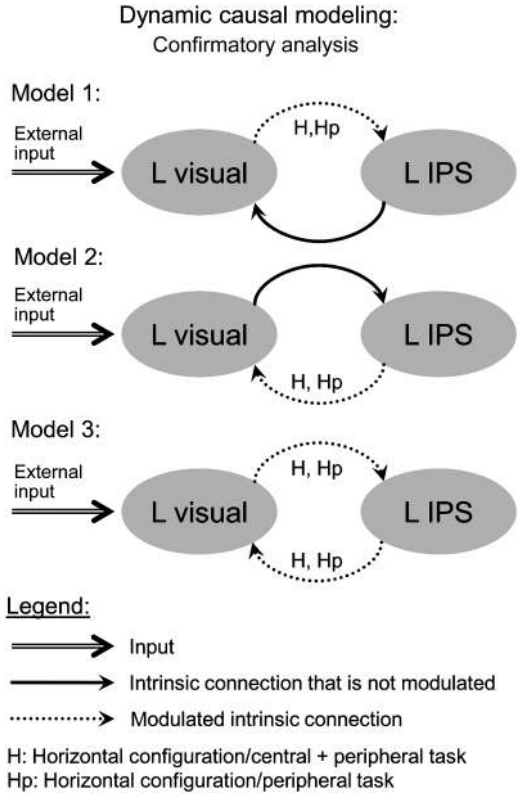

Figure 3. DCM: Confirmatory analysis. Three models for the DCM model comparison. The GLM used to extract the relevant time series for the 3 DCMs consisted of the external input term and 2 regressors: Horizontal configuration (H) and horizontal configuration/peripheral task (Hp). Same conventions as in Figure 2.

In the color patch experiment (Fig. 1*A*), there was a significant main effect of stimulus display (d': $F_{2,18} = 13.22$, $P < 0.001$; RTs: $F_{1.3,11.6} = 27.96$, G–G adj. $P < 0.001$; Fig. 4*E*,*F*): Subjects responded significantly more slowly ($F_{1,9} = 32.17$, $P < 0.001$) and less accurately ($F_{1,9} = 17.19$, $P = 0.003$) when a distracter was added to the display, compared with the target only condition. Furthermore, d' was lower when target and distracter were configured along the horizontal relative to the vertical axis ($F_{1,9} = 7.09$, $P = 0.03$).

All subjects fixated well, according to on-line infrared eye tracking.

fMRI Experiments: Behavioral Data

In the main fMRI experiment (Fig. 1*B*), the main effect of task (2 levels: Central task, peripheral task) (d': $F_{1,21} = 15.46$, $P < 0.001$; RTs: $F_{1,21} = 2.88$, $P = 0.10$) and the main effect of stimulus display (3 levels: Single grating, horizontal configuration, vertical configuration; d': $F_{2,42} = 17.32$, $P < 0.001$; RTs: $F_{2,42} = 15.46$, $P < 0.001$) were significant. The interaction between task and stimulus display was also significant (d': $F_{2,42} = 15.36$, $P < 0.001$; RTs: $F_{2,42} = 19.96$, $P < 0.001$; Fig. 4*C*,*D*). Subjects were less accurate and slower when a distracter was added to the peripheral target but not during the central task (planned interaction contrast, d': $F_{1,21} = 31.16$, $P < 0.001$; RTs: $F_{1,21} = 33.56$, $P < 0.001$). Under double-stimulation conditions, the interaction between configuration axis and task was not significant (d': $F_{1,21} = 0.62$, $P = 0.44$; RTs: $F_{1,21} = 1.95$, $P = 0.18$; Fig. 4*C*,*D*). The number of saccades into the right upper quadrant did not differ between conditions according to a 2-way repeated-measures ANOVA with task and stimulus display as factors (main effect of task: $F_{1,21} = 2.91$, $P = 0.10$; main effect of stimulus display: $F_{1,21} = 0.33$, $P = 0.72$; interaction between task and stimulus display: $F_{1,21} = 0.71$, $P = 0.50$). Overall, the number of saccades per condition per run was low (mean ± standard error of the mean: 1.18 ± 0.41).

In the sensory fMRI experiment, we did not observe an effect of peripheral stimulation on performance during the central letter detection task (d': $F_{3,15} = 1.25$, $P = 0.33$; RTs: $F_{3,15} = 1.44$, $P = 0.27$; d': 3.13 ± 28; RTs: 771 ± 39). The

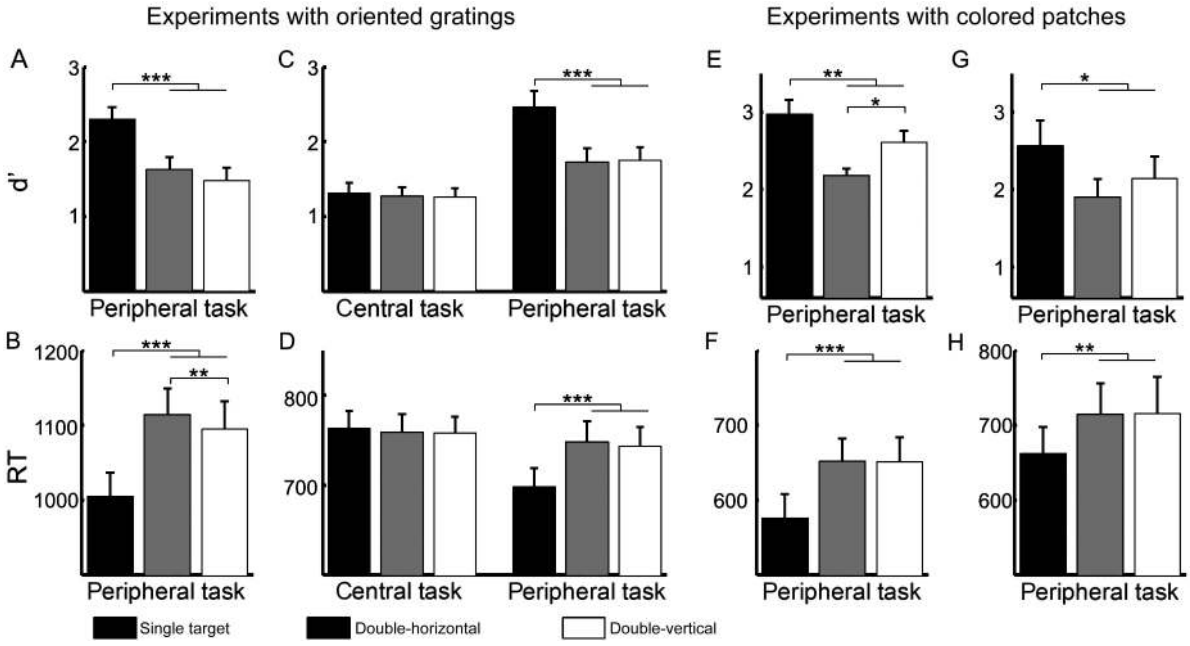

Figure 4. Behavioral performance. Mean *d′* score (*A*,*C*,*E*,*G*) and mean RT (*B*,*D*,*F*,*H*) as a function of the stimulus display. Performance is given for the first behavioral experiment with oriented gratings (*A* and *B*), the main fMRI experiment (*C* and *D*), and for the experiments with colored patches (second behavioral experiment [*E* and *F*] and color fMRI experiment [*G* and *H*]). Error bars indicate 1 standard error of the mean across subjects.

number of saccades into the right upper quadrant did not differ between conditions ($F_{3,15} = 1.67$, $P = 0.22$; average number of saccades per condition per run: 2.63 ± 0.79).

In the hemifield fMRI experiment, there was no main effect of hemifield on performance (d': $F_{1,4} = 2.10$, $P\ P = 0.22$; RTs: $F_{1,4} = 0.52$, $P = 0.51$). Neither did the main effect of configuration axis on accuracy (d': $F_{1,4} = 0.14$, $P = 0.73$) or RTs ($F_{1,4} = 4.09$, $P = 0.11$) reach significance. There was no interaction between hemifield and configuration axis (d': $F_{1,4} = 0.72$, $P = 0.44$; RTs: $F_{1,4} = 0.57$, $P = 0.49$). The number of saccades into the right upper quadrant or the left upper quadrant, respectively, did not differ between conditions according to a 2-way repeated-measures ANOVA with hemifield and configuration as factors.

In the color fMRI experiment (Fig. 1*D*), the main effect of stimulus display (3 levels: Single color patch, horizontal configuration, vertical configuration) was significant for d' ($F_{2,10} = 4.43$, $P = 0.04$) and RTs ($F_{2,10} = 17.15$, $P = 0.001$): Performance was worse on double compared with single-stimulation trials (d': $F_{1,5} = 6.83$, $P = 0.05$); RTs: $F_{1,5} = 26.27$, $P = 0.004$; Fig. 4*G*,*H*). Performance was not modulated by the configuration axis between target and distracter (d': $F_{1,5} = 1.25$, $P = 0.31$; RTs; $F_{1,5} < .0.001$, $P = 0.99$). The number of saccades into the right upper quadrant did not differ between conditions according to a repeated-measures ANOVA ($F_{2,10} = 1.24$, $P = 0.33$; average number of saccades per condition per run: 1.08 ± 0.64).

Functional MRI

Main fMRI Experiment

In the presence of 2 peripheral gratings, activity levels in left and right IPS and FEF were higher when attention was oriented toward the peripheral gratings compared with the central attention condition (contrast 1: Effect of task; Fig. 5*A*; Table 1A). Activity in right IPS, left and right FEF, and right middle frontal gyrus was higher when the 2 peripheral grating were configured along the horizontal compared with the vertical axis (contrast 2: Effect of configuration axis; Fig. 5*B*–*E*; Table 1C), with a smaller cluster of activation in left IPS (left IPS: $x = -30$, $y = -69$, $z = 33$; $Z = 4.29$, 41 voxels). There was a significant interaction between task and configuration axis (contrast 3) in left IPS, left FEF, and the dorsomedial prefrontal cortex (DMPFC; Table 1D, Fig. 5*F*). In addition, we observed smaller clusters of activation in right IPS (9, −69, 48, $Z = 3.48$, 28 voxels) and right FEF (33, 0, 63, $Z = 3.88$, 34 voxels). We further evaluated the simple effects of which this interaction was composed: When subjects performed the peripheral orientation discrimination task, activity was higher when target and distracter were configured along the horizontal compared with the vertical axis (Fig. 5*G*–*I*; contrast 4; left IPS: $t_{21} = 4.81$, uncorrected $P < 0.0001$; left FEF: $t_{21} = 5.20$, uncorrected $P < 0.0001$; DMPFC: $t_{21} = 3.86$, uncorrected $P = 0.0009$; right IPS: $t_{21} = 2.81$, uncorrected $P = 0.01$, right FEF: $t_{21} = 5.56$, uncorrected $P < 0.0001$). In the central letter detection task, activity levels in these regions did not significantly differ between horizontal and vertical configuration (contrast 5; uncorrected $P > 0.24$).

We further tested statistically any differences between left and right IPS with regards to the effect of configuration axis. To select the left and right IPS voxels in an unbiased manner, we contrasted all double-stimulation conditions to all single-stimulation conditions across the 2 tasks (contrast 6; voxel-level $P < 0.005$ and FWE-corrected cluster-level $P < 0.05$). This yielded a left and a right middle IPS VOI, with an extent of 327 and 180 voxels, respectively (Fig. 6*A*). We averaged the responses across all voxels in each VOI and conducted an ANOVA with hemispheric side (2 levels: Left vs. right IPS),

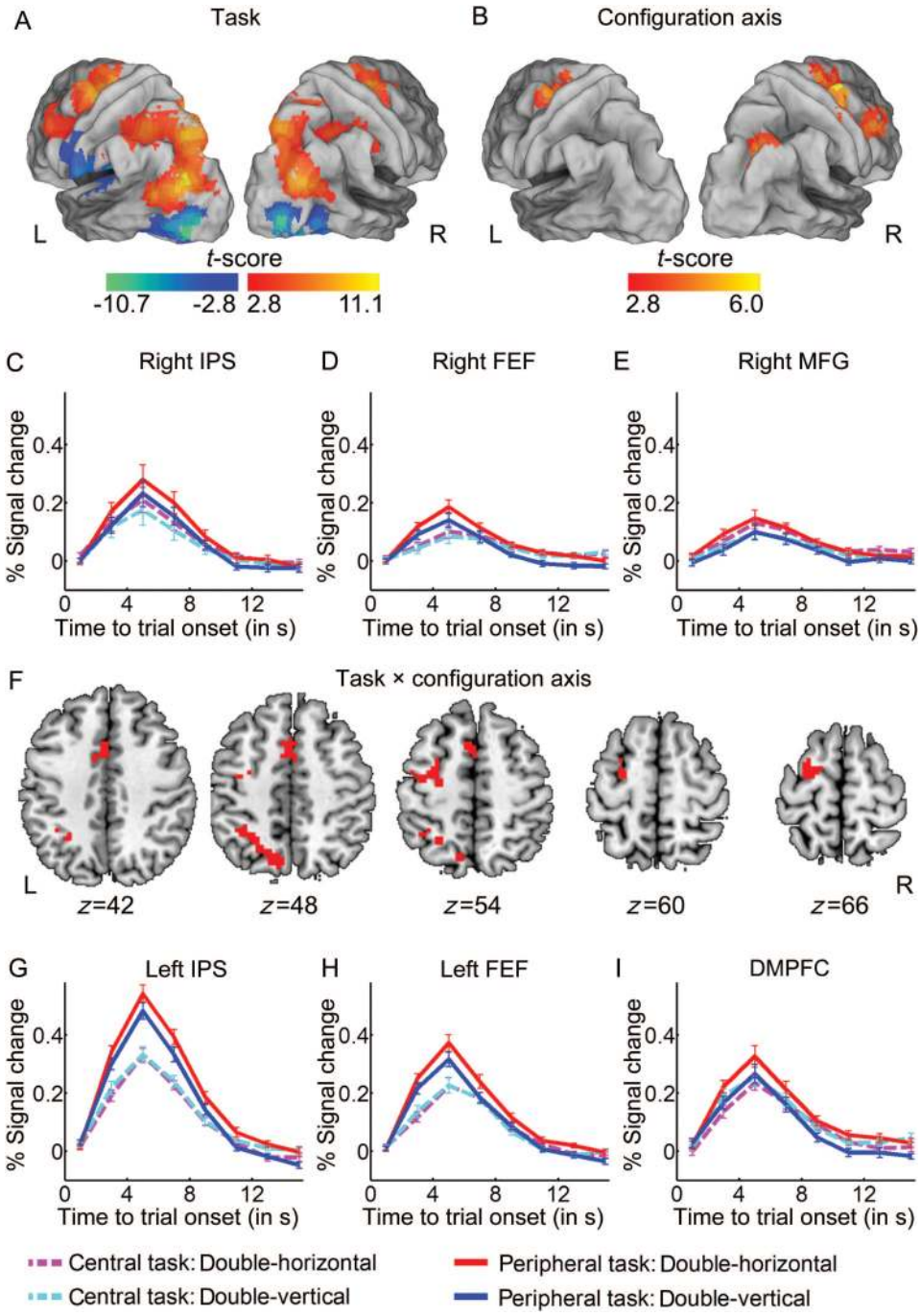

Figure 5. Main fMRI experiment. (*A*) *T*-map for the effect of task in case of double stimulation (contrast 1: Peripheral task minus central task; red to yellow) and the reverse (blue to cyan). The *T*-map is projected onto a surface rendering of the brain (population averaged, landmark- and surface-based [PALS] atlas, Caret 5.612 [Van Essen, 2005]). Threshold: Voxel-level uncorrected $P < 0.005$, cluster-level FWE-corrected $P < 0.05$. (*B*) *T*-map for the effect of configuration axis (contrast 2: Double horizontal minus double vertical). (*C–E*) Time-activity curves averaged over all subjects and all significant voxels in right IPS (*C*), right FEF (*D*), and right MFG (*E*), defined based on contrast 2. Error bars indicate 1 standard error of the mean across subjects. (*F*) *T*-map for the interaction between task and configuration axis (contrast 3), projected onto axial slices of the brain. (*G–I*) Time-activity curves averaged over all subjects and all significant voxels in left IPS (*G*), left FEF (*H*), and DMPFC (*I*), defined based on contrast 3. IPS, intraparietal sulcus; FEF, frontal eye fields; DMPFC, dorsomedial prefrontal cortex; MFG, middle frontal gyrus.

task (2 levels: Central vs. peripheral), and stimulus configuration (2 levels: Horizontal vs. vertical configuration). There was a significant main effect of hemisphere ($F_{1,21} = 9.89$, $P = 0.005$), task ($F_{1,21} = 79.14$, $P < 0.0001$), and configuration axis ($F_{1,21} = 16.70$, $P = 0.0005$), without 2-way interactions ($P > 0.21$). There was a significant 3-way interaction between hemisphere, task, and configuration ($F_{1,21} = 15.70$, $P = 0.0007$): The effect of configuration axis in the peripheral task was significant in left IPS ($P = 0.0006$) without any effect of configuration axis in the central task ($P = 0.53$), yielding a significant interaction between task and configuration axis ($F_{1,21} = 4.04$, $P = 0.06$). In the right IPS, the effect of configuration axis was also significant in the peripheral ($P = 0.03$) task, but not in the central task ($P = 0.10$), but the interaction between task and

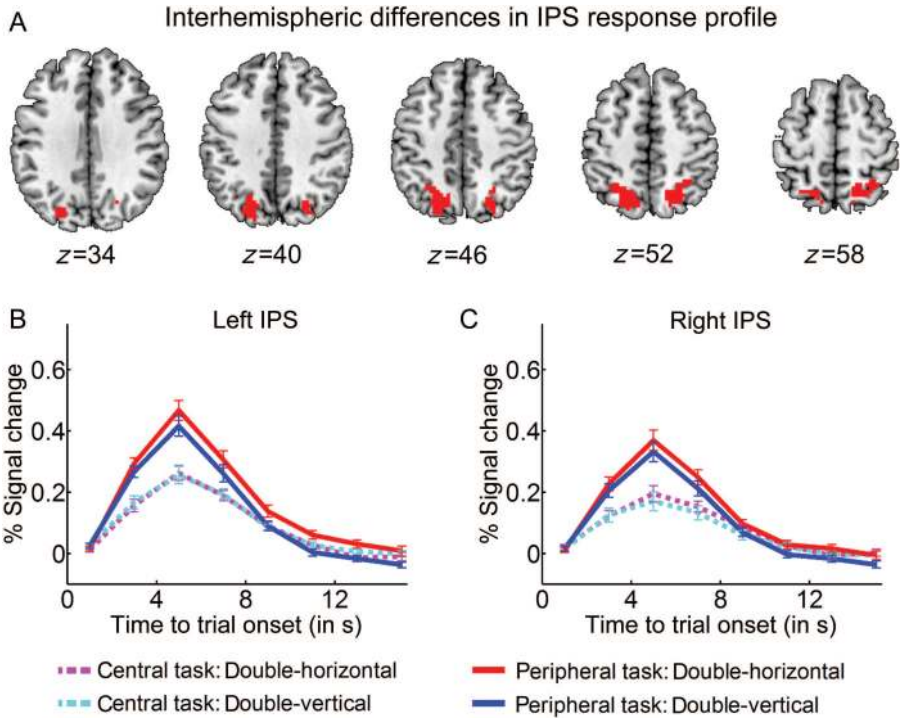

Figure 6. Interhemispheric differences in IPS response profile. (*A*) *T*-map for the contrast of all double versus all single-stimulation conditions (contrast 6, threshold: Voxel-level uncorrected $P < 0.005$, FWE-corrected $P < 0.05$), projected onto axial slices of the brain. (*B* and *C*) Time-activity curves averaged over all subjects and all significant voxels in left IPS (*B*) and right IPS (*C*), defined based on contrast 6. Error bars indicate 1 standard error of the mean across 22 subjects.

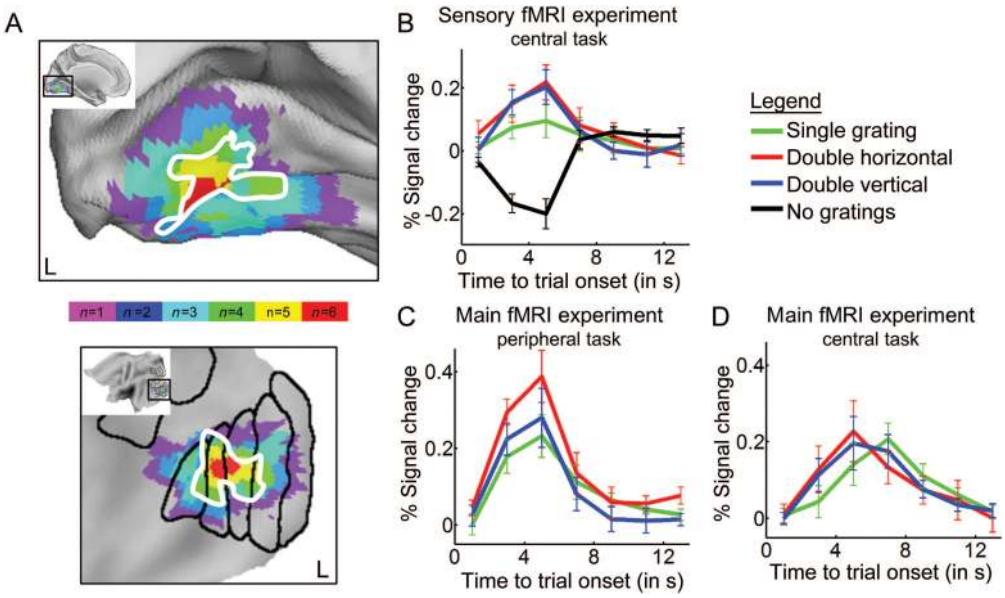

Figure 7. Sensory fMRI experiment. (*A*) *T*-maps for the effect of adding gratings to the display in the central letter detection task (contrast 8). Threshold: Single-subject, FWE-corrected $P < 0.05$. The color-scale indicates the number of subjects for which the *t*-map survived the threshold. The black borders outline the visuotopic cortical partitioning scheme available in Caret (PALS atlas, Caret 5.612 [Van Essen 2005]). The white border reflects the area significant in a random effects analysis across 6 subjects (voxel-level uncorrected $P < 0.001$, cluster-level corrected $P < 0.05$). (*B*) Time-activity curves averaged over all 6 subjects and voxels in the subject-specific VOIs, using the data from the sensory fMRI experiment. (*C* and *D*) Time-activity curves averaged over all subjects and voxels in the subject-specific VOIs, using the data from the main fMRI experiment (*C*: Peripheral orientation discrimination task; *D*: Central letter detection task). Error bars indicate 1 standard error of the mean across subjects.

configuration axis remained below the significance threshold ($P = 0.59$; Fig. 6*B*,*C*). This analysis indicates that the interaction between task and configuration axis was significantly stronger in left than in right IPS.

Effects in Extrastriate Cortex

In each subject, we defined a VOI containing the voxels in occipital cortex that showed a visual response to the gratings (contrast 8; FWE-corrected $P < 0.05$; Fig. 7*A*; Table 2A). The

occipital areas that responded to the peripheral gratings encompassed V2v, VP, V4, and V8 based on the visuotopic cortical partitioning scheme available in Caret (Van Essen 2005; Fig. 7*A*). Under central attention conditions, this response did not depend on the configuration axis (horizontal vs. vertical; $t_5 = 0.68$, $P = 0.52$; Fig. 7*B*). Next, we extracted the time courses in these VOIs using the data from the same subjects in the main fMRI experiment. We observed a significant interaction between task and configuration axis ($F_{1,5} = 20.65$, $P = 0.006$): Activity was increased for a horizontal relative to a vertical configuration axis when subjects performed the peripheral orientation discrimination task ($t_5 = 4.98$, $P = 0.004$; Fig. 7*C*), but not when attention was focused on the central letter stream ($t_5 = 1.33$, $P = 0.24$; Fig. 7*D*).

Hemifield fMRI Experiment

In the hemifield fMRI experiment, the main effect of configuration axis on left IPS activity levels was significant ($F_{1,29} = 4.63$, $P = 0.04$). The effect of hemifield ($F_{1,29} = 0.68$, $P = 0.41$) and the interaction between configuration axis and hemifield ($F_{1,29} = 2.54$, $P = 0.12$) did not reach significance.

Color fMRI Experiment

When subjects performed a color discrimination task on colored patches presented in the upper right quadrant, the BOLD response in left IPS was higher when target and distracter were configured along the horizontal relative to the vertical configuration axis ($t_5 = 3.76$, $P = 0.01$).

DCM: Main Analysis

We formally compared (Penny et al. 2004) 6 models (Fig. 2), which described the effective connectivity between left IPS (Fig. 5*F*,*G*; Table 1D) and left visual cortex (Fig. 7*A*, delineated in white; Table 2B). The outcome of the model comparison was highly in favor of model 2 above all other models. The GBF in favor of model 2 compared with any alternative model was 2.56×10^{17} or higher (Penny et al. 2004; Table 3). Compared with the model where we replaced the horizontal configuration/peripheral task and the vertical configuration/peripheral task with the corresponding central task conditions (model 5), the evidence in favor of model 2 was overwhelming (GBF = 1.6×10^{187}): In 17 of the 22 subjects, the evidence in favor of model 2 compared with model 5 was very strong (BF $\geq$ 150), in only one of the subjects, there was weak evidence in favor of model 5 ($1 <$ BF < 3), and in the remaining 4 subjects either positive or strong evidence in favor of model 2.

Table 4 summarizes the average rate constants (in Hertz), as estimated using model 2, for the external input (Table 4A), the intrinsic connections (Table 4B), and the modulatory effects (Table 4C). The strength of the intrinsic connection from visual cortex to IPS was significantly stronger than that of the intrinsic connection from the IPS to the visual cortex ($t_{21} = 3.31$, $P = 0.003$; Table 4B). The double-stimulation peripheral attention conditions (Hp and Vp) significantly enhanced the feedback connection from the IPS to the visual cortex (Table 4C). This connectivity enhancement was significantly stronger for double stimulation compared with single stimulation/peripheral task (Sp), both in case of a horizontal (Hp vs. Sp: $t_{21} = 5.04$, $P < 0.0001$) and of a vertical configuration axis (Vp vs. Sp: $t_{21} = 4.28$, $P = 0.0003$). The strength of the modulation did not differ depending on the configuration axis (Hp vs. Vp: $P = 0.99$).

Table 3
Bayesian selection of dynamic causal models: Main analysis

Models compared	GBF	PER	Weak evidence	No decision
Model 2 versus model 1	2.51×10^{23}	15:5	2:0	0
Model 2 versus model 3	2.56×10^{17}	13:0	2:0	7
Model 2 versus model 4	8.21×10^{204}	20:0	2:0	0
Model 2 versus model 5	1.56×10^{187}	21:0	0:1	0
Model 2 versus model 6	7.23×10^{197}	21:0	1:0	0

Note: The GBF is the product of the BF over the 22 subjects. The PER is the number of subjects in which evidence is positive in favor of model 2 rather than the alternative model, compared with the number of subjects in which evidence is positive in favor of the alternative model rather than model 2. Positive evidence is defined as a BF higher than 3. Fourth column: The number of subjects in which weak evidence favors model 2 rather than the alternative model (BF between 1 and 3), compared with the number of subjects with weak evidence in favor of the alternative model. Last column: The number of subjects in which the AIC and BIC disagreed about which model was superior and no decision could be made.

Table 4
Main DCM analysis

Connections	Rate constants	SEM	*P*-values
(A) External input			
Input to visual	0.026	0.006	**0.0003**
(B) Intrinsic connectivity			
Visual to IPS	0.846	0.229	**0.002**
IPS to visual	0.235	0.065	**0.001**
(C) Modulatory effects on feedback connection			
Single target/peripheral task	0.147 (63%)	0.068	0.04
Horizontal configuration/peripheral task	0.369 (157%)	0.074	<**0.0001**
Vertical configuartion/peripheral task	0.369 (157%)	0.072	<**0.0001**

Note: Parameter estimates for model 2. (A) Rate constants for the rate of change of neuronal activity (Hz) induced by the external input. Values in bold are significant after Bonferroni correction for multiple comparisons. *P*-values are based on a 1-sample *t*-test. (B) Average rate constants (Hz) over subjects for the intrinsic connections. This reflects the impact that 1 VOI exerts over the other VOI on the basis of the overall experimental context rather than in relation to a specific experimental condition. (C) Changes in connection strength from the IPS to the extrastriate VOI during the peripheral task with a single target, the peripheral task with the target and the distracter configured along the horizontal axis or along the vertical axis. Rate constants are expressed in real values and in percentage change relative to the intrinsic connectivity. SEM, standard error of the mean.

DCM: Confirmatory Analysis

In our confirmatory DCM analysis (Fig. 3), all subjects had a local maximum in left middle IPS and left extrastriate cortex which were sufficiently close to the group maximum (mean coordinates ± standard deviation across 22 subjects; left IPS: $x = -26 \pm 8$, $y = -55 \pm 6$, $z = 50 \pm 4$; left extrastriate cortex: $x = -20 \pm 5$; $y = -76 \pm 6$; $z = -11 \pm 5$). The average size of the nodes in left middle IPS and left extrastriate cortex was 28 ± 5 and 24 ± 7 voxels, respectively. These extrastriate and IPS individual VOIs were defined based on a contrast 7. Each showed a significant interaction effect between task and configuration axis (contrast 3).

The outcome of the model comparison was again highly in favor of model 2 above models 1 and 3 (Table 5; GBF > 5.16×10^{10}). Table 6 summarizes the average rate constants, as estimated using model 2. Consistent with the main DCM comparison (Table 4), the horizontal configuration between 2 gratings significantly enhanced the feedback connection from the IPS to the visual cortex during the peripheral task only (Table 6C, Hp).

Discussion

Activity levels in left and right middle IPS were higher when stimuli were configured along the horizontal versus the

Table 5
Bayesian selection of dynamic causal models: Confirmatory analysis

Models compared	GBF	PER	Weak evidence	No decision
Model 2 versus model 1	3.91×10^{17}	13.2	3:4	0
Model 2 versus model 3	5.16×10^{10}	12:0	5:1	4

Note: Terminology and abbreviations (see Table 3).

Table 6
Confirmatory DCM analysis

Connections	Rate constants	SEM	*P*-values
(A) External input			
Input to visual	0.273	0.004	<**0.0001**
(B) Intrinsic connectivity			
Visual to IPS	0.945	0.198	**0.0001**
IPS to visual	0.246	0.042	<**0.0001**
(C) Modulatory effects on feedback connection			
Horizontal configuration	−0.042 (−17%)	0.034	0.22
Horizontal configuration/peripheral task	0.273 (110%)	0.047	<**0.0001**

Note: Parameter estimates for model 2. (A) Rate constants for the rate of change of neuronal activity (Hz) induced by the external input. (B) Average rate constants (Hz) over subjects for the intrinsic connections. (C) Changes in connection strength from the IPS to the extrastriate VOI during horizontal configuration trials and during peripheral task trials with horizontal configuration. Values in bold are significant after Bonferroni correction for multiple comparisons. SEM, standard error of the mean.

vertical configuration axis (Fig. 5*B*,*C*,*F*,*G*), but only when the stimuli were relevant for the task (Fig. 5*F*,*G*). This interaction between task and configuration axis was also observed in upstream visual areas that responded to the stimuli (Fig. 7*A*). The feedback connection from left middle IPS to these upstream visual areas was enhanced when attention was directed toward the peripheral stimuli and a distracter was added (Figs 2 and 3, model 2; Tables 4 and 6). This modulatory effect of a distracter was specific for the peripheral attention conditions (Tables 4*C* and 6*C*). The effect of configuration axis in IPS was also observed when the peripheral stimuli consisted of color patches and subjects performed a color discrimination. With respect to our original research question, these data indicate that the effect of configuration axis is an attentional effect originating at the level of the attentional priority map rather than the visual sensory map.

In the behavioral experiments, performance during the peripheral attention task was consistently worse when the 2 competing stimuli were arranged along the horizontal compared with the vertical axis, in accordance with earlier studies (Molenberghs et al. 2008). This effect of configuration axis on accuracy or RTs was not seen in the main fMRI experiment. The main fMRI and the behavioral experiment mainly differed in the presentation of the letter stream and the addition of the central letter detection task. Due to this letter stream, stimulus onset asynchrony was longer in the fMRI than in the behavioral experiment. The letter stream started before grating onset and continued until after grating offset. We introduced the central letter detection task in the fMRI so that we could test the interaction between task and display. The introduction of the central letter detection task and the presence of a central letter stream during the peripheral task may have negatively affected the sensitivity of the classical behavioral measures for detecting the effect of configuration axis, despite the fact that fMRI was still able to detect an effect of configuration axis during peripheral attention conditions. The behavioral effect of configuration axis was also not significant in the hemifield and the color fMRI control experiments, but this is likely due to the small sample size ($n = 5$ and 6, respectively). Despite the absence of any behavioral difference, the IPS activity difference between the horizontal and the vertical configuration peripheral conditions persisted similarly to previous fMRI experiments (Molenberghs et al. 2008). The effect of configuration axis on IPS activity levels is therefore not contingent on differences in task difficulty.

The peripheral and central attention conditions differed in the direction of attention (toward the gratings vs. away from the gratings) and the nature of the task (orientation discrimination vs. letter identification). Because of the multiple differences between the central and the peripheral attention conditions, the main effect of task (central vs. peripheral attention) is relatively aspecific in terms of cognitive processes. The principal contrast that addresses our original research question (Fig. 5*F*,*G*) is based on the interaction between task and the spatial configuration between stimuli. This interaction effect is free of differences in sensory stimulation: In each run, each of the 4 possible stimulus locations was occupied equally often in the double-horizontal as in the double-vertical conditions. Across trials, these 2 conditions were therefore sensorially matched within each run.

The interaction between task and configuration axis was significantly stronger in left than in right middle IPS (Fig. 6). This IPS segment, which we call the middle or horizontal segment of IPS, lies anterior to the IPS segment that is visually responsive and sensitive to the direction of attention called IPS0/1 (Vandenberghe et al. 2005, 2012; Gillebert et al. 2011). The stronger interaction effect in left compared with right middle IPS probably reflects a higher degree of endogenous control needed to select between the 2 stimuli when they are aligned horizontally. This interpretation is in line with an attentional origin of the configuration effect. Left middle IPS has been implicated relatively more in endogenous control compared with right IPS (Vandenberghe et al. 1997; Kim et al. 1999). In one of our previous studies (Molenberghs et al. 2008), we focused on the effect of configuration axis on right middle IPS because of the overlap with the right-sided ischemic lesions in patients with spatial–attentional deficits (Molenberghs et al. 2008). In that study as in the current study, both left and right middle IPS showed an effect of configuration axis during the peripheral task (Molenberghs et al. 2008). Alternatively, the hemispheric laterality of middle IPS involvement may have been influenced by the right-sided presentation of the stimuli. A control experiment where stimuli were presented either in left or right upper quadrant could not confirm this possibility. For that reason, we consider it more likely that the relative preponderance of the left compared with the right middle IPS relates to relatively high endogenous control requirements.

The effect of configuration axis is independent of the reference orientation of the gratings (Molenberghs et al. 2008). We used right oblique orientations to minimize long-range interactions between grating orientations (Polat and Sagi 1994; Pavlovskaya et al. 1997). Critically, when we used color patches and a color discrimination task, the effect of configuration axis was confirmed, both with respect to performance (Fig. 4*E*) and activity levels in the middle segment of left and right IPS. The effect of configuration axis therefore is not

restricted to the use of gratings. A similar effect of configuration axis for various sorts of stimuli during peripheral attention has been observed in studies of crowding (He et al. 1996, 1997; Strasburger 2005; Feng et al. 2007; Livne and Sagi 2011). When a target is surrounded by neighboring distracters (flankers), visual discrimination of the target becomes more difficult (Eriksen and Eriksen 1974; He et al. 1996; Feng et al. 2007; Levi 2008; Whitney and Levi 2011). Crowding is stronger when the target and distracters are horizontally rather than vertically aligned within a same quadrant (Feng et al. 2007), and this cannot be explained by any differences in visual acuity between the 2 dimensions, horizontal versus vertical (Feng et al. 2007). Although the exact neural mechanisms of crowding remain a subject of research (Levi 2008; Whitney and Levi 2011), similar mechanisms may be responsible for the effect of configuration axis in crowding and that observed in the current study. Crowding shares many characteristics with the effects observed here, including a difference along the horizontal compared with the vertical dimension, high target-distracter similarity, and peripheral viewing. One substantial difference, however, is that a close target-flanker proximity is a prerequisite for crowding (Toet and Levi 1992; Pelli et al. 2004; Whitney and Levi 2011), while, in the context of spatial cueing paradigms, distracters modulate performance even when target and distracter are presented at a wider distance (Geeraerts et al. 2005; Vandenberghe et al. 2005; Molenberghs et al. 2008; Gillebert et al. 2011).

When we restricted our search volume to the voxels that showed a visual response to the peripheral gratings, we could detect an effect of configuration axis in extrastriate cortex too but only when subjects directed attention to the peripheral gratings (Fig. 7*B–D*). During the peripheral attention conditions, the feedback connection from the IPS to the extrastriate cortex was also enhanced by the addition of a distracter to the peripheral target grating. We have previously demonstrated that the addition of an irrelevant distracter to a target leads to activity increases in middle IPS (Vandenberghe et al. 2005; Molenberghs et al. 2008), implying middle IPS in the resolution of competition between simultaneously presented stimuli (Vandenberghe and Gillebert 2009). Our connectivity analysis provides direct evidence for the mechanism through which middle IPS exerts this role, through top-down control of extrastriate areas processing the peripheral stimuli. This is in accordance with evidence that attentional variables can modulate the functional connectivity between IPS and extrastriate cortex (Bressler et al. 2008; Desseilles et al. 2009; Lauritzen et al. 2009; Chadick and Gazzaley 2011; Davranche et al. 2011). These studies manipulated attention by varying the task demands, while in our study the enhancement of the feedback connection was purely induced by varying the spatial configuration between stimuli. According to diffusion tensor imaging studies, human IPS is structurally connected with extrastriate visual areas through the inferior fronto-occipital fasciculus (Uddin et al. 2010). In monkeys, the lateral intraparietal area, the putative homolog of middle IPS (Sereno et al. 2001), has reciprocal cortico-cortical connections with many extrastriate visual areas, including areas V3, V3A, and V4 (Blatt et al. 1990). The modulatory effect on the connection between extrastriate cortex and IPS did not differ between the horizontal and the vertical configuration conditions. We suggest that in the presence of an effect of the configuration axis at the regional level, this effect can be transmitted to regions at a distance even when connectivity strength remains the same for the 2 types of stimulus configuration axis.

Our findings lead us to the hypothesis that in the attentional priority map, the differential weighting of attentional priorities between targets and distracters requires more attentional resources when the 2 stimuli are on a same horizontal axis rather than a vertical axis. This may contribute to the pervasive effect of horizontal stimulus configurations in studies of lateralized spatial–attentional deficits. Spatial–attentional deficits due to unilateral lesions are expressed far more often along the horizontal rather than the vertical gradient. In a previous study (Molenberghs et al. 2008), we applied a similar paradigm in patients with unifocal cortical lesions: The spatial cue directed attention to one visual quadrant, and the target grating appeared in that quadrant together with an irrelevant grating in an un-cued quadrant. Patients with a right inferior parietal lesion are significantly more impaired during contralesional versus ipsilesional orienting when stimuli are configured along the same horizontal axis than when they occupy diagonally opposite quadrants or 2 quadrants within the same hemifield. This is also true when stimuli are positioned within the same quadrant, identically to the manipulation used in the current study (Molenberghs et al. 2008).

To conclude, the spatial configuration between target and distracter influences activity levels in middle IPS and extrastriate cortex, indicative of an asymmetry within the attentional priority map between the horizontal and the vertical dimension. The presence of competing stimuli not only increases middle IPS activity (Vandenberghe et al. 2005; Molenberghs et al. 2008) but also the feedback connection from the IPS to the extrastriate cortex. Our findings fit with a model where the middle IPS segment plays a critical role in calibrating attentional priorities and influences early visual processing through its feedback connections to extrastriate cortex (Pessoa et al. 2003; Yantis and Serences 2003; Yantis 2008; Vandenberghe and Gillebert 2009).

Funding

This work was supported by Research Foundation Flanders (FWO), Flanders, Belgium (G0668.07 ESF EuroCores Program); Katholieke Universiteit Leuven (OT/08/56), and Federaal Wetenschapsbeleid belspo (Inter-University Attraction Pole; P6/29). C.R.G. is a PhD fellow and R.V. a senior clinical investigator of the FWO. J.W. is supported by a Methusalem grant from the Flemish Government (METH/08/02).

Notes

Conflict of Interest: None declared.

References

Bisley JW, Goldberg ME. 2010. Attention, intention, and priority in the parietal lobe. Annu Rev Neurosci. 33:1–21.

Blatt GJ, Andersen RA, Stoner GR. 1990. Visual receptive field organization and cortico-cortical connections of the lateral intraparietal area (area LIP) in the macaque. J Comp Neurol. 299:421–445.

Bressler SL, Tang W, Sylvester CM, Shulman GL, Corbetta M. 2008. Top-down control of human visual cortex by frontal and parietal cortex in anticipatory visual spatial attention. J Neurosci. 28:10056–10061.

Bundesen C. 1990. A theory of visual-attention. Psychol Rev. 97:523–547.
Buschman TJ, Miller EK. 2007. Top-down versus bottom-up control of attention in the prefrontal and posterior parietal cortices. Science. 315:1860–1862.
Chadick JZ, Gazzaley A. 2011. Differential coupling of visual cortex with default or frontal-parietal network based on goals. Nat Neurosci. 14:830–832.
Davranche K, Nazarian B, Vidal F, Coull J. 2011. Orienting attention in time activates left intraparietal sulcus for both perceptual and motor task goals. J Cogn Neurosci. 23:3318–3330.
Desseilles M, Balteau E, Sterpenich V, Dang-Vu TT, Darsaud A, Vandewalle G, Albouy G, Salmon E, Peters F, Schmidt C et al. 2009. Abnormal neural filtering of irrelevant visual information in depression. J Neurosci. 29:1395–1403.
Di Pellegrino G, De Renzi E. 1995. An experimental investigation on the nature of extinction. Neuropsychologia. 33:153–170.
Dupont P, Gillebert CR, Nelissen N, Vandenberghe R. 2011. Dynamical causal modeling of fMRI time series at 3T: effect of the magnetic field mismatch. In: Front neuroinform conference abstract: 4th INCF congress of neuroinformatics, Boston, USA.
Eriksen B, Eriksen C. 1974. Effects of noise letters upon the identification of a target letter in a nonsearch task. Percept Psychophys. 16:143–149.
Feng C, Jiang Y, He S. 2007. Horizontal and vertical asymmetry in visual spatial crowding effects. J Vis. 7:13.1–1310.
Friston K, Harrison L, Penny W. 2003. Dynamic causal modelling. Neuroimage. 19:1273–1302.
Geeraerts S, Lafosse C, Vandenbussche E, Verfaillie K. 2005. A psychophysical study of visual extinction: ipsilesional distractor interference with contralesional orientation thresholds in visual hemineglect patients. Neuropsychologia. 43:530–541.
Gilbert CD, Wiesel TN. 1989. Columnar specificity of intrinsic horizontal and cortico-cortical connections in cat visual cortex. J Neurosci. 9:2432–2442.
Gilbert CD, Wiesel TN. 1990. The influence of contextual stimuli on the orientation selectivity of cells in primary visual cortex of the cat. Vision Res. 30:1689–1701.
Gillebert CR, Mantini D, Thijs V, Sunaert S, Dupont P, Vandenberghe R. 2011. Lesion evidence for the critical role of the intraparietal sulcus in spatial attention. Brain. 134:1694–1709.
He S, Cavanagh P, Intriligator J. 1997. Attentional resolution. Trends Cogn Sci. 1:115–121.
He S, Cavanagh P, Intriligator J. 1996. Attentional resolution and the locus of visual awareness. Nature. 383:334–337.
Hung J, Driver J, Walsh V. 2011. Visual selection and the human frontal eye fields: effects of frontal transcranial magnetic stimulation on partial report analyzed by bundesen's theory of visual attention. J Neurosci. 31:15904–15913.
Hung J, Driver J, Walsh V. 2005. Visual selection and posterior parietal cortex: effects of repetitive transcranial magnetic stimulation on partial report analyzed by bundesen's theory of visual attention. J Neurosci. 25:9602–9612.
Itti L, Koch C. 2000. A saliency-based search mechanism for overt and covert shifts of visual attention. Vision Res. 40:1489–1506.
Kastner S, Nothdurft HC, Pigarev IN. 1997. Neuronal correlates of pop-out in cat striate cortex. Vision Res. 37:371–376.
Kim Y, Gitelman D, Nobre A, Parrish T, LaBar K, Mesulam MM. 1999. The large-scale neural network for spatial attention displays multifunctional overlap but different asymmetry. Neuroimage. 9:269–277.
Kraft A, Kehrer S, Hagendorf H, Brandt SA. 2011. Hemifield effects of spatial attention in early human visual cortex. Eur J Neurosci. 33:2349–2358.
Lauritzen TZ, D'Esposito M, Heeger DJ, Silver MA. 2009. Top-down flow of visual spatial attention signals from parietal to occipital cortex. J Vis. 9:18.1–1814.
Levi DM. 2008. Crowding–an essential bottleneck for object recognition: a mini-review. Vision Res. 48:635–654.
Livne T, Sagi D. 2011. Multiple levels of orientation anisotropy in crowding with Gabor flankers. J Vis. 11:18.
Macmillan N, Creelman C. 1991. Detection theory: a user's guide. Cambridge (UK): Cambridge University Press.
Malach R, Amir Y, Harel M, Grinvald A. 1993. Relationship between intrinsic connections and functional architecture revealed by optical imaging and in vivo targeted biocytin injections in primate striate cortex. Proc Natl Acad Sci USA. 90:10469–10473.
Mesulam MM. 1981. A cortical network for directed attention and unilateral neglect. Ann Neurol. 10:309–325.
Mildner T, Norris DG, Schwarzbauer C, Wiggins CJ. 2001. A qualitative test of the balloon model for BOLD-based MR signal changes at 3T. Magn Reson Med. 46:891–899.
Molenberghs P, Gillebert CR, Peeters R, Vandenberghe R. 2008. Convergence between lesion-symptom mapping and functional magnetic resonance imaging of spatially selective attention in the intact brain. J Neurosci. 28:3359–3373.
Monosov IE, Thompson KG. 2009. Frontal eye field activity enhances object identification during covert visual search. J Neurophysiol. 102:3656–3672.
Pavlovskaya M, Sagi D, Soroker N, Ring H. 1997. Visual extinction and cortical connectivity in human vision. Cereb Cortex. 6:159–162.
Pelli DG, Palomares M, Majaj NJ. 2004. Crowding is unlike ordinary masking: distinguishing feature integration from detection. J Vis. 4:1136–1169.
Penny WD, Stephan KE, Mechelli A, Friston KJ. 2004. Comparing dynamic causal models. Neuroimage. 22:1157–1172.
Pessoa L, Kastner S, Ungerleider LG. 2003. Neuroimaging studies of attention: from modulation of sensory processing to top-down control. J Neurosci. 23:3990–3998.
Polat U, Mizobe K, Pettet MW, Kasamatsu T, Norcia AM. 1998. Collinear stimuli regulate visual responses depending on cell's contrast threshold. Nature. 391:580–584.
Polat U, Sagi D. 1994. Spatial interactions in human vision: from near to far via experience-dependent cascades of connections. Proc Natl Acad Sci USA. 91:1206–1209.
Raftery A. 1995. Sociological methodology, chapter Bayesian model selection in social research. Cambridge (MA): Blackwell. p. 111–163.
Sereno MI, Pitzalis S, Martinez A. 2001. Mapping of contralateral space in retinotopic coordinates by a parietal cortical area in humans. Science. 294:1350–1354.
Stephan KE, Marshall JC, Penny WD, Friston KJ, Fink GR. 2007. Interhemispheric integration of visual processing during task-driven lateralization. J Neurosci. 27:3512–3522.
Strasburger H. 2005. Unfocused spatial attention underlies the crowding effect in indirect form vision. J Vis. 5:1024–1037.
Thompson KG, Biscoe KL, Sato TR. 2005. Neuronal basis of covert spatial attention in the frontal eye field. J Neurosci. 25:9479–9487.
Toet A, Levi DM. 1992. The two-dimensional shape of spatial interaction zones in the parafovea. Vision Res. 32:1349–1357.
Ts'o DY, Gilbert CD, Wiesel TN. 1986. Relationships between horizontal interactions and functional architecture in cat striate cortex as revealed by cross-correlation analysis. J Neurosci. 6:1160–1170.
Uddin LQ, Supekar K, Amin H, Rykhlevskaia E, Nguyen DA, Greicius MD, Menon V. 2010. Dissociable connectivity within human angular gyrus and intraparietal sulcus: evidence from functional and structural connectivity. Cereb Cortex. 20:2636–2646.
Vandenberghe R, Duncan J, Dupont P, Ward R, Poline J, Bormans G, Michiels J, Mortelmans L, Orban GA. 1997. Attention to one or two features in left or right visual field: a positron emission tomography study. J Neurosci. 17:3739–3750.
Vandenberghe R, Geeraerts S, Molenberghs P, Lafosse C, Vandenbulcke M, Peeters K, Peeters R, Van Hecke P, Orban GA. 2005. Attentional responses to unattended stimuli in human parietal cortex. Brain. 128:2843–2857.
Vandenberghe R, Gillebert CR. 2009. Parcellation of parietal cortex: convergence between lesion-symptom mapping and mapping of the intact functioning brain. Behav Brain Res. 199:171–182.
Vandenberghe R, Molenberghs P, Gillebert CR. 2012. Spatial attention deficits in humans: the critical role of superior compared to inferior parietal lesions. Neuropsychologia. 50:1092–1103.
Van Doren L, Dupont P, De Grauwe S, Peeters R, Vandenberghe R. 2010. The amodal system for conscious word and picture

identification in the absence of a semantic task. Neuroimage. 49:3295–3307.
Van Essen DC. 2005. A Population-Average, Landmark- and Surface-based (PALS) atlas of human cerebral cortex. Neuroimage. 28:635–662.
Wager TD, Nichols TE. 2003. Optimization of experimental design in fMRI: a general framework using a genetic algorithm. Neuroimage. 18:293–309.
Wardak C, Ibos G, Duhamel JR, Olivier E. 2006. Contribution of the monkey frontal eye field to covert visual attention. J Neurosci. 26:4228–4235.
Whitney D, Levi DM. 2011. Visual crowding: a fundamental limit on conscious perception and object recognition. Trends Cogn Sci. 15:160–168.
Woldorff M, Hazlett C, Fichtenholtz H, Weissman D, Dale A, Song A. 2004. Functional parcellation of attentional control regions of the brain. J Cogn Neurosci. 16:149–165.
Yantis S. 2008. The neural basis of selective attention: cortical sources and targets of attentional modulation. Curr Dir Psychol Sci. 17:86–90.
Yantis S, Serences JT. 2003. Cortical mechanisms of space-based and object-based attentional control. Curr Opin Neurobiol. 13:187–193.